

## Controllable bistabilities and bifurcations in a photoexcited GaAs/AlAs superlattice

K. J. Luo, S. W. Teitsworth,<sup>a)</sup> H. Kostial, and H. T. Grahn<sup>b)</sup>

*Paul-Drude-Institut für Festkörperelektronik, Hausvogteiplatz 5–7, D-10117 Berlin, Germany*

N. Ohtani

*ATR-ACRL, 2-2 Hikaridai Seika-cho, Soraku-gun, Kyoto 619-0288, Japan*

(Received 23 March 1999; accepted for publication 28 April 1999)

Self-sustained photocurrent oscillations and bifurcation processes have been experimentally investigated in an undoped, photoexcited GaAs/AlAs superlattice by varying the laser intensity. Within a certain range of laser intensities, a bistability of the photocurrent can be observed in the photocurrent versus voltage characteristics. The width of the bistability region can be controlled by varying the laser intensity. In the bistable regime, the photocurrent oscillations disappear via a subcritical Hopf bifurcation with increasing applied voltage. Outside this regime, the transition from oscillations to a static state is a supercritical Hopf bifurcation for lower laser intensities, while at higher laser intensities a homoclinic connection is observed. © 1999 American Institute of Physics. [S0003-6951(99)03125-3]

Resonant tunneling in weakly coupled superlattices (SLs) results in negative differential conductivity (NDC) regions in the current density versus electric field characteristics.<sup>1–4</sup> Because of these NDC regions, the SL becomes a nonlinear system exhibiting nonlinear phenomena such as electric-field domain formation with a static or oscillating domain boundary.<sup>1–4</sup> Under domain formation, the electric field in the SL breaks up into two regions of constant field, which are separated by a domain boundary.<sup>1–4</sup> It has been shown that domain formation is greatly affected by the carrier density in the SL. If the carrier density falls below a critical value, the domain formation will become unstable, and self-sustained current oscillations will appear.<sup>1–5</sup> In recent years, current oscillations have been observed in doped SLs.<sup>4</sup> A number of interesting dynamical phenomena such as bistability<sup>6</sup> as well as driven and undriven chaos<sup>7,8</sup> have been observed. However, the effect of the carrier density on these dynamical phenomena is experimentally not well known, since the carrier density cannot be easily varied in a doped SL. Recently, self-sustained oscillations were observed in undoped, photoexcited SLs, where the carrier density can be tuned by varying the intensity of the exciting laser.<sup>9,10</sup>

In this letter, we report measurements on an undoped, photoexcited SL that show the effect of the carrier density on the transition between static and oscillating domains. The carrier density will be varied within *a single sample* by changing the illumination intensity. For intermediate laser intensities, a bistable region is observed near the edge of the first photocurrent (PC) plateau in the time-averaged PC-V characteristics. The width of the bistable region can be controlled by changing the laser intensity. In the bistable regime, the oscillations disappear via a subcritical Hopf bifurcation with increasing direct-current (dc) bias. For low (high) laser intensity, the bistability region disappears, and a supercritical

Hopf bifurcation (homoclinic connection) describes the transition from the oscillating to the static state. These are experimental results on the use of carrier density variation to control the bifurcation type and the bistability in a nonlinear solid state system.

The investigated sample consists of a 100-period, weakly coupled SL with 6.2 nm GaAs wells and 3.4 nm AlAs barriers grown by molecular beam epitaxy on a (100)  $n^+$ -type GaAs substrate. The SL is undoped and embedded in a  $p^+ - i - n^+$  structure. For a more detailed description of the structures, see Ref. 9. The sample is etched to yield mesas with a diameter of 120  $\mu\text{m}$ . The dc bias is applied perpendicular to the SL layers. A continuous-wave (cw) He-Ne laser (632.8 nm) with a maximum power of 21.3 mW is focused at normal incidence onto the  $p^+$ -cap layer to excite carriers in the SL region. The laser power will be used throughout the letter to indicate the respective photocurrent. The experimental data are recorded in a He-flow cryostat at 6.4 K using high-frequency coaxial cables with a bandwidth of 20 GHz. The power spectra of the photocurrent oscillations are detected with an Advantest R3361 spectrum analyzer. The real-time traces of the photocurrent are recorded with a LeCroy LC574AL digital oscilloscope. In the experiments, negative voltages refer to a negative bias applied to the  $p^+$  top layer, i.e., reverse bias for the  $p^+ - i - n^+$  diode.

Figure 1 shows the time-averaged PC-V characteristics at 6.4 K for several laser powers. At 21.3 mW, a plateau is observed from about  $-1.45$  to  $-8.88$  V. This plateau exists for all laser powers shown in Fig. 1, but its width depends on the laser power. For laser powers below 1 mW, the plateau is replaced by a smooth NDC behavior as shown in the inset to Fig. 1. This NDC region is induced by the detuning of the resonant alignment of subbands in the SL, as demonstrated previously by theoretical and experimental investigations.<sup>1–4</sup> For domain formation, an NDC region and a sufficiently large carrier density are required.<sup>1–4</sup> At 1 mW, the excited carrier density in the SL is still too low for the formation of electric-field domains. In this case, no plateau in the PC-V

<sup>a)</sup>Permanent address: Department of Physics, Duke University, Box 90305, Durham, NC 27708-0305.

<sup>b)</sup>Electronic mail: htg@pdi-berlin.de

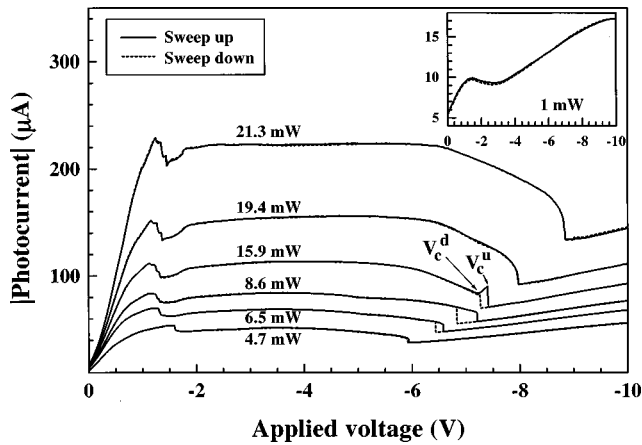


FIG. 1. Time-averaged PC-V characteristics at 6.4 K for several laser powers as indicated. The inset shows the PC-V characteristics for 1 mW. The sweep directions are indicated by different lines.

characteristics and no oscillations in the time domain are observed. However, for larger laser powers, domain formation should occur as indicated by the presence of the photocurrent plateau shown in Fig. 1. At the same time, self-sustained photocurrent oscillations appear in the time domain.<sup>9</sup> With increasing laser power, the carrier density becomes larger, and the electric-field domains exist over a larger bias voltage range so that the plateau covers a wider voltage region as shown in Fig. 1. Within the range of laser powers used here, we do not observe the formation of stationary domains, where branch-like structures should appear in the plateaus.<sup>3,11</sup>

Within a certain range of laser powers, a bistability region of the photocurrent is observed near the edge of the plateau as shown for 6.5, 8.6, and 15.9 mW in Fig. 1. When the reverse bias is increased, the photocurrent jumps down at a critical voltage of  $V_c^u$ . At the same time, the oscillations disappear. When the reverse bias is decreased, the photocurrent jumps up at a critical voltage of  $V_c^d$ , and the oscillations reappear. The width of the bistable region can be controlled by changing the laser power. Figure 2 shows the relationship between the laser power and the critical voltages  $V_c^u$  as well as  $V_c^d$ . At low laser powers, there is no bistability. With increasing laser power, the bistable region appears, and its

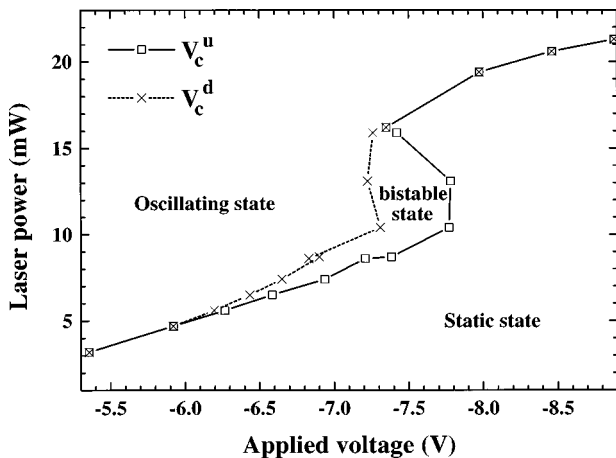


FIG. 2. The relationship between the critical voltages  $V_c^u$  and  $V_c^d$  (cf. Fig. 1) and the laser power at 6.4 K. The lines between the data points are a guide to the eye.

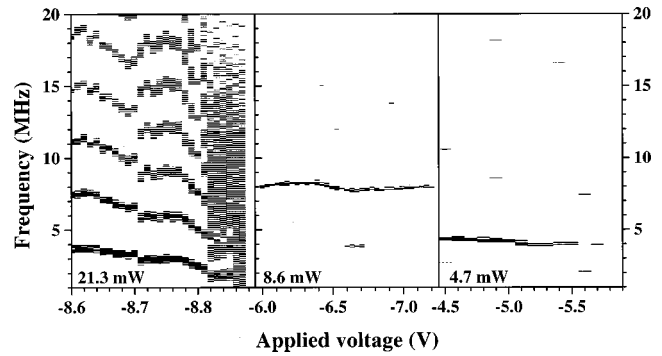


FIG. 3. Power spectra of the photocurrent oscillations recorded at 6.4 K for laser powers of 21.3, 8.6, and 4.7 mW. The darker areas correspond to larger amplitudes.

width increases gradually until a laser power of 13.1 mW is reached. With a further increase of the laser power, the bistable region rapidly collapses. Finally, the bistability disappears, when the laser power is larger than 16.2 mW. Figure 2 represents a phase diagram, separating the oscillating from the static state. The region enclosed by the dashed and solid lines indicates the bistable region, where the oscillating and the static states coexist.

By tuning the laser power, not only the bistability, but also the bifurcation type from the oscillating to the static state can be controlled. Figure 3 shows some typical power spectra of the photocurrent oscillations as a function of reverse bias voltage recorded in the sweep-up direction. In this work, we are only interested in the voltage region just before the oscillations disappear. At 21.3 mW, the frequency decreases gradually to zero with increasing reverse bias (the spectrum becomes broadband just before the oscillations completely disappear). At the same time, the amplitude of the oscillation hardly changes as shown for the real-time traces at  $-8.70$  and  $-8.85$  V in Fig. 4(a). Such a behavior indicates that the oscillations disappear via a homoclinic connection, i.e., the oscillations vanish with a fixed amplitude and zero frequency without any bistability.<sup>12-14</sup> The broadband spectrum observed very close to the transition point results from the extreme sensitivity of the system near the saddle point of a homoclinic orbit, and is generally expected for homoclinic connections. With decreasing laser power, this type of bifurcation remains until the bistability appears in the PC-V characteristics. In the bistable regime, the oscillations are found to disappear via a subcritical Hopf bifurcation,<sup>6,13,14</sup> i.e., the oscillations vanish with a finite amplitude and a finite frequency as shown in Fig. 3 for 8.6 mW (the static state is reached at  $-7.21$  V). There are two critical points for a subcritical Hopf bifurcation. At one critical point, the bifurcation takes place from an unstable focus (i.e., static state) to a stable focus and an unstable limit cycle (i.e., periodic oscillations), while at the other critical point the unstable limit cycle merges into a stable limit cycle. Bistability should be present between these two critical points (cf. Ref. 15). This type of bifurcation exists until the bistability region vanishes again at lower laser power. In the low power regime, the oscillations disappear via a supercritical Hopf bifurcation,<sup>13-16</sup> i.e., with increasing reverse bias the oscillation amplitude shrinks to zero, while the frequency remains at a finite value. This behavior can be seen in the power

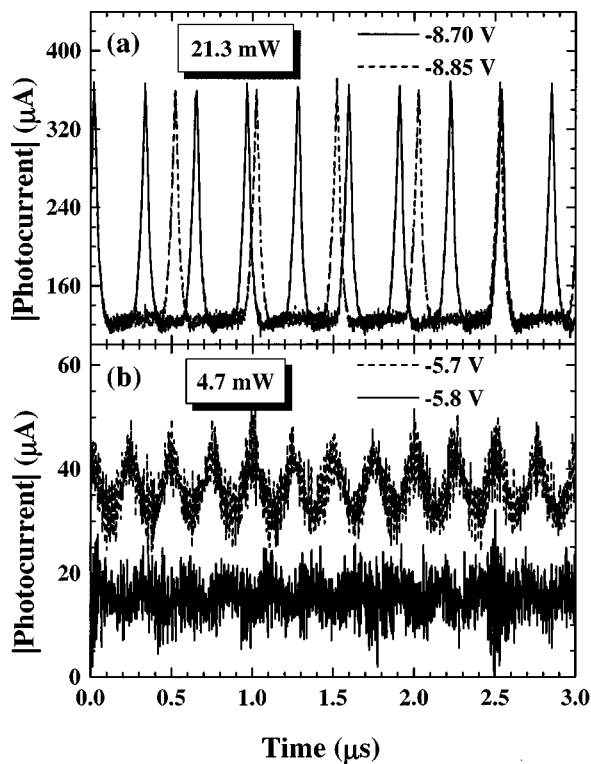


FIG. 4. Real-time photocurrent traces at 6.4 K before the oscillations disappear for laser powers of (a) 21.3 and (b) 4.7 mW. The applied voltages are indicated in the figure. For clarity, the trace at  $-5.8$  V for 4.7 mW has been shifted downwards by  $20 \mu\text{A}$ .

spectra in Fig. 3 for 4.7 mW and the real-time traces in Fig. 4(b). For a supercritical Hopf bifurcation, there is only one critical point, where an unstable focus and a stable limit cycle change into a stable focus. No hysteresis should be present.<sup>15,16</sup>

Bistability and different bifurcation scenarios have already been predicted in theoretical work on doped as well as undoped, photoexcited SLs.<sup>4,5,13,14</sup> By changing both the dc bias and the carrier density, the theoretical investigations have revealed very complex dynamical phenomena, which are due to the strong nonlinearity in this system. Although the SLs studied theoretically do not have the same parameters as our sample, we have demonstrated the existence of bistability and three different bifurcation scenarios in these experiments. We expect quantitative agreement between theory and experiment, when theoretical work is carried out using parameters appropriate for the experimental samples.

In summary, the evolution from a static state at low carrier densities to an oscillating domain at higher carrier densities has been demonstrated in an undoped, photoexcited SL by increasing the laser power. We have observed a controllable bistability and several distinct bifurcation scenarios. In the bistable regime, the oscillations disappear via a subcritical Hopf bifurcation with increasing reverse bias. When the bistability is absent at low (high) laser powers, the oscillations disappear via a supercritical Hopf bifurcation (homoclinic connection).

The authors would like to thank K. Tominaga for sample growth. Partial support of the Deutsche Forschungsgemeinschaft within the framework of Sfb 296 is gratefully acknowledged.

<sup>1</sup>L. L. Bonilla, in *Nonlinear Dynamics and Pattern Formation in Semiconductors and Devices*, edited by F.-J. Niedernostheide (Springer, Berlin, 1995), Chap. 1.

<sup>2</sup>A. Wacker, in *Theory of Transport Properties of Semiconductor Nanostructures*, edited by E. Schöll (Chapman and Hall, London, 1998), Chap. 10.

<sup>3</sup>H. T. Grahn, in *Hot Electrons in Semiconductors, Physics and Devices*, edited by N. Balkan (Clarendon, Oxford, 1998), pp. 357–382.

<sup>4</sup>J. Kastrop, R. Hey, K. H. Ploog, H. T. Grahn, L. L. Bonilla, M. Kindelan, M. Moscoso, A. Wacker, and J. Galán, *Phys. Rev. B* **55**, 2476 (1997).

<sup>5</sup>E. Schöll, G. Schwarz, M. Patra, and A. Wacker, in *Hot Carriers in Semiconductors*, edited by K. Hess, J. P. Leburton, and U. Ravaioli (Plenum, New York, 1996), p. 177; F. Prengel, M. Patra, G. Schwarz, and E. Schöll, in *Proceeding of the 23rd International Conference on the Physics of Semiconductors*, edited by M. Scheffler and R. Zimmermann (World Scientific, Singapore, 1997), p. 1667.

<sup>6</sup>Y. Zhang, R. Klann, K. H. Ploog, and H. T. Grahn, *Appl. Phys. Lett.* **70**, 2825 (1997).

<sup>7</sup>Y. Zhang, J. Kastrop, R. Klann, K. H. Ploog, and H. T. Grahn, *Phys. Rev. Lett.* **77**, 3001 (1996); Y. Zhang, R. Klann, H. T. Grahn, and K. H. Ploog, *Superlattices Microstruct.* **21**, 565 (1997).

<sup>8</sup>K. J. Luo, H. T. Grahn, K. H. Ploog, and L. L. Bonilla, *Phys. Rev. Lett.* **81**, 1290 (1998).

<sup>9</sup>N. Ohtani, M. Hosoda, and H. T. Grahn, *Appl. Phys. Lett.* **70**, 375 (1997).

<sup>10</sup>N. Ohtani, N. Egami, H. T. Grahn, K. H. Ploog, and L. L. Bonilla, *Phys. Rev. B* **58**, R7528 (1998).

<sup>11</sup>H. T. Grahn, H. Schneider, and K. von Klitzing, *Phys. Rev. B* **41**, 2890 (1990).

<sup>12</sup>R. Döttling and E. Schöll, *Phys. Rev. B* **45**, 1935 (1992).

<sup>13</sup>M. Moscoso, J. Galán, and L. L. Bonilla (unpublished).

<sup>14</sup>M. Moscoso, L. L. Bonilla, and J. Galán, in *Proceeding of the 24th International Conference on the Physics of Semiconductors* (World Scientific, Singapore, 1999).

<sup>15</sup>P. Bergé, Y. Pomeau, and C. Vidal, *Order Within Chaos* (Wiley, New York, 1984), Chap. II.

<sup>16</sup>M. P. Shaw, V. V. Mitin, E. Schöll, and H. L. Grubin, *The Physics of Instabilities in Solid State Electron Devices* (Plenum, New York, 1992), Chap. 1, pp. 21–26.